PROCESSING OF HIGH PERFORMANCE FLUOROPOLYMERS BY LASER SINTERING

Carlo Campanelli, Ricky D. Wildman, Christopher J. Tuck

Faculty of Engineering, The University of Nottingham, University Park, Nottingham, NG7 2RD, UK

Abstract

One of the main limitations of laser sintering (LS) is its narrow material portfolio. Fluoropolymers are a family of polymers with outstanding properties such as wide service temperatures (−260 °C - +260 °C), excellent resistance to chemicals, sunlight, flames, and weathering without the addition of stabilizers, plasticizers or fillers. In this study, fluoropolymers such as perfluoroalkoxy (PFA) and polychlorotrifluoroethylene (PCTFE) have been used in laser sintering. PFA and PCTFE have melting temperatures of 304 °C and 210 °C respectively which make them challenging to process. Our results demonstrate the feasibility of these materials in LS and that warping was the major issue encountered due to the relatively low powder bed temperature of ~182 °C. We illustrate how particle size, additives, and thermal conditioning affect the powder flow and how the warping can be decreased by utilizing a modified build plate, and different scan strategies and part orientations. Flat sheets were successfully produced with potential use in membrane-based applications.

Introduction

It is well-known that additive manufacturing (AM), and more specifically laser sintering (LS), has great potential but several limitations, one of which is the narrow material portfolio [1]; of the over tens of thousands of different polymers available for injection molding, less than 30 of them are suitable for being laser sintering [2].

Thanks to their outstanding properties such as wide service temperatures (roughly −260°C +260°C), and excellent resistance to chemicals, sunlight, flames and weathering without the addition of stabilizers, plasticiser or fillers, fluoropolymers have been widely used in automotive, electrical and chemical industries, as well in medical devices and aircraft [3]. While any one of these properties can be found in other materials, fluoropolymers are matchless when two or more of these properties are needed in the same application [4]. Fluoropolymers gain their peculiar properties from the strong C-F bond (~480 kJ/mol, the strongest known single bond in organic chemistry), which also increases the C-C bond strength by roughly 100 kJ/mol compared to that found in hydrocarbons (~360 kJ/mol) [5]. This increase in bond energy is due to the high electronegativity of the fluorine atoms. In fact, the fluorine atoms, with their bigger size (compared to hydrogen atoms), shield the carbon backbone of the polymer, increasing its chemical resistance. The combination of strong bond energies, size, and the electronegativity of fluorine atoms is the basis for the properties of fluoropolymers. With the exception of polytetrafluoroethylene (PTFE) and polyvinyl fluoride (PVF), all fluoropolymers are melt processable [3] and only a few are soluble in common solvents at room temperature, including Teflon AF, THV, PVDF, and CYTOP.

The literature about the use of fluoropolymer in AM is quite limited and mainly focused on polyvinylidene fluoride-trifluoroethylene P(VDF-TrFE) and its piezoelectric properties in material jetting [6]–[10], FDM [11], [12], and laser sintering [13], [14]. 3M recently announced a way to 3D Print PTFE through SLA with promising initial results [15].

This study investigates for the first time, the use of polychlorotrifluoroethylene (PCTFE) and perfluoroalkoxy (PFA) in laser sintering. PCTFE and PFA maintain excellent performance over an extensive temperature range, from −240 to 200 °C [4] and from −196 °C to 260 [3], respectively. The investigation starts with a study of the thermal properties of the two polymers with a focus on the crystallisation temperature, isothermal crystallisation time at different temperatures, and effect of additives on crystallisation. Next, the particle size distribution and flow behaviour of the powders were analysed with and without the presence of additives, and after several thermal treatments. Finally, the powders were sintered in an EOS Formiga P100. The major issue encountered was warping, due to the relatively low powder bed temperature (~182 °C), and the high porosity, due to the high viscosities and low bulk densities of the polymers, especially for the PCTFE powder. As a result of these limitations only small parts are printable but membrane-based applications could be possible thanks to the high thermal and chemical stability of fluoropolymers. Finally, the use of a modified build plate showed promise and allowed the printing of multiple layers.

Materials and Methods

Materials
PCTFE powder (Chemical Point UG) and PFA ACX-31S powder (Daikin) were used. PCTFE has a melt flow index (MFI) of 0.97 g/10min (as stated by the supplier) and an average particle size below 1 μm. PFA has a melt flow index of 25 g/10min (ASTM D3307, as reported by the supplier) and an average particle size of 24 μm. MONARCH 800 Carbon Black and CAB-O-SIL Untreated Fumed Silica (both from Cabot Corporation) were used as flowing agents. Powders and additives were mixed in polypropylene containers roughly 1 kg at a time. The mixing was done with stainless steel blades at ~1000 RPM for several hours.

Laser sintering apparatus
A commercially available LS machine (EOS Formiga P100) was used. This machine uses a CO_2 laser which operates at a wavelength around 10.6 μm with a spot size of 420 μm and a nominal power of 30 W. The maximum scan velocity is 5000 mm/s while the working volume is 200 x 250 x 350 mm. The maximum powder bed temperature is 182 °C. The layers are deposited with a doctor blade. The areal energy density (ED) was calculated with the following equation:

$$ED = \frac{laser\ power}{scan\ velocity * hatching\ space}$$ (Eq.1)

Thermal characterization
The thermal characterization was conducted with a DSC 8000 (PerkinElmer). The samples were weighted with a Kern ABT 100-5m scale and aluminum pans were used. The PCTFE R01 weighed 8.2 g while the PCTFE with 1 wt% carbon black (CB) weighed 8.6 g. The PFA R01 sample weighed 7.4 g while the PFA with 0.2 wt% carbon black weighed 8.6 g. The same samples were utilized for the isothermal crystallization experiments. The crystallization and melting peaks were calculated with heating/cooling rate of 20 °C/min over a range of 0-230 °C and 0-330 °C for PCTFE and PFA, respectively. The PCTFE isothermal crystallization was measured by holding the temperature at 230 °C for 3 minutes with subsequent cooling at 40 °C/min to 180 °C and by finally holding the temperature at 180 °C for roughly 20-25 minutes. At this point the sample was heated back to 230 °C with a rate of 100 °C/min and all the previous steps repeated. At each repeat, the holding temperature was changed to 182-184-186-190 °C for both pure PCTFE and PCTFE

with 1 wt% CB. Similarly, the PFA isothermal crystallization was measured by holding the temperature at 330 °C for 2 minutes with subsequent cooling at 40 °C/min to 276 °C and held for roughly 20-25 minutes. At this point the sample was heated back to 330 °C with a rate of 100 °C/min and all the previous steps repeated at 276-278-280-282-284-286-288 °C for the pure PFA powder and 284-286-288-290-292-294 °C for the PFA with 0.2 wt% CB. Higher temperatures were used for PFA 0.2 wt% CB because at lower temperatures the crystallization was happening too quickly. All the reported values were obtained from calculations within the PerkinElmer Pyris software v11.1.0.0488. The crystallization activation energy was calculated by plotting the natural logarithm of the isothermal crystallization peak time (time passed from the reaching of the isothermal temperature to the crystallization peak) against the reverse of the temperature in Kelvin multiplied by 1000. The DSC scans were repeated twice for the determination of the melting and crystallization temperatures (at 20 °C/min) and once for the determination of the isothermal crystallization.

Density measurement

The density of the printed parts was calculated by measuring the volume and weight of the parts. The weight was measured with a Kern ABT 100-5m scale. The volume of the parts was calculated by measuring the dimensions of the parts with a caliper and a micrometer.

Thermal treatment

Samples were prepared by filling 250 ml beakers with roughly 40 g of PCTFE powder. Each sample was then subject to a different thermal treatment in an oven. The thermal treatments were 4 hours at 200 °C, 205 °C, and 210 °C, and 24 hours at 210 °C. Afterwards, the powders were ground with a pestle and mortar.

Particle size distribution

The particle size distribution was obtained using a Mastersizer 3000 (Malvern, UK) with the Hydro EV accessory for wet analyses and the Aero S accessory for dry analyses. Particles were assumed non-spherical for the PFA powder and spherical for the PCTFE powder based on the SEM images. Refractive index and absorption index were assigned values of 1.43 and 0.002 for both polymers [16], [17]. In the wet analyses, deionized water was used as a dispersant, and a refractive index of 1.330 was employed. The reported particle size distribution values were obtained from calculations within the Mastersizer software.

FT4 powder flowability

The flowability of the powders and conditioned bulk density (CBD) were measured with an FT4 powder rheometer (Freeman Technology). The tests were done using 25 ml glass vessels and the Stability & Variable Flow Rate Method. This method measures several parameters but the ones reported here are the Specific Energy (SE) and CBD. The SE is normalized against mass and measured in mJ/g. SE is used to determine the flowability of a powder in a low stress environment. Generally, values below 5 mJ/g are associated with low cohesion, while values above 10 mJ/g are associated with high cohesion. The measured bulk density is called conditioned because the instrument executes a conditioning cycle to remove external influences and increase repeatability. The conditioning establishes a low stress, homogeneous packing state. The majority of the measurements were repeated 3 times but some of measurements were done only once because of the high repeatability given by the instrument. By way of comparison Ziegelmeier et al. [18] tested the quality of the data obtained with the FT4 to a Revolution Powder Analyzer and the Hausner Ratio.

Scanning electron microscopy

Scanning Electron Microscopy (SEM) images were obtained using a TM3030 tabletop SEM (Hitachi High Technologies, USA). The samples were fixed on adhesive carbon tabs.

Experimental results

Thermal characterization

The DSC curves for the PCTFE powder showed the presence of a wide processing window of 40 °C between the melting peak (210.72 ± 0.15 °C) and the re-crystallization peak (170.43 ± 0.32 °C) (Figure 1a). For comparison, PA12 has a broad processing window of 38 °C [19]. The presence of 1 wt% CB did not visibly affect the melting temperature (210.94 ± 0.01 °C) but it did shift the re-crystallization peak to a higher temperature (173.09 ± 0.01 °C) (Figure 1a). The isothermal crystallization in Figure 1c shows that the crystallization was happening relatively quickly, even at 10-20 °C above the crystallization temperature. The crystallization peaks decreased in height and increased in width as the isothermal temperature increased. Under isothermal conditions, the presence of 1 wt% CB increased the crystallization speed by roughly 52%. The activation energy of the crystallization was not affected by the presence of 1 wt% CB, as showed in Figure 1e. The activation energy equation for PCTFE and PCTFE + 1 wt% CB were $y = -47.495x + 104.79$ and $y = -47.048x + 103.38$, respectively. The gradients of these equations multiplied by the gas constant gave activation energies of 394.9 and 391.2 kJ/mol, respectively. Overall, these results suggest that a powder bed temperature above 190 °C is required: at that temperature, 50% of the crystallization happened after 11.4 and 6.9 minutes when PCTFE was used without and with CB, respectively.

The DSC curves for the PFA powder also showed the presence of a relatively wide processing window of 32 °C between the melting peak (304.10 ± 0.57 °C) and the crystallization peak (271.93 ± 0.17 °C) (Figure 1b). The presence of 0.2 wt% CB did not visibly affect the melting temperature (304.13 ± 0.13 °C) but it did shift the crystallization peak to a higher temperature (276.96 ± 0.09 °C) (Figure 1b). The isothermal crystallization in Figure 1d for the neat PFA shows that the crystallization was happening relatively quickly, even at 20 °C above the crystallization temperature. At equal temperatures, the presence of 0.2 wt% CB increases the crystallization speed by roughly 10 times. The activation energy of the crystallization was slightly affected by the presence of 0.2 % CB, as shown in Figure 1d. The activation energy equations for PFA and PFA + 0.2 wt% CB were $y = -75.881x + 137.26$ and $y = -82.849x + 147.3$, respectively. These correspond to activation energies of 630.9 and 688.8 kJ/mol, respectively. In summary, these results suggest that a powder bed temperature above 288 °C is required for PFA: at that temperature, 50% of the crystallization happened in less than 10 minutes for both neat PFA and PFA + 0.2 wt% CB.
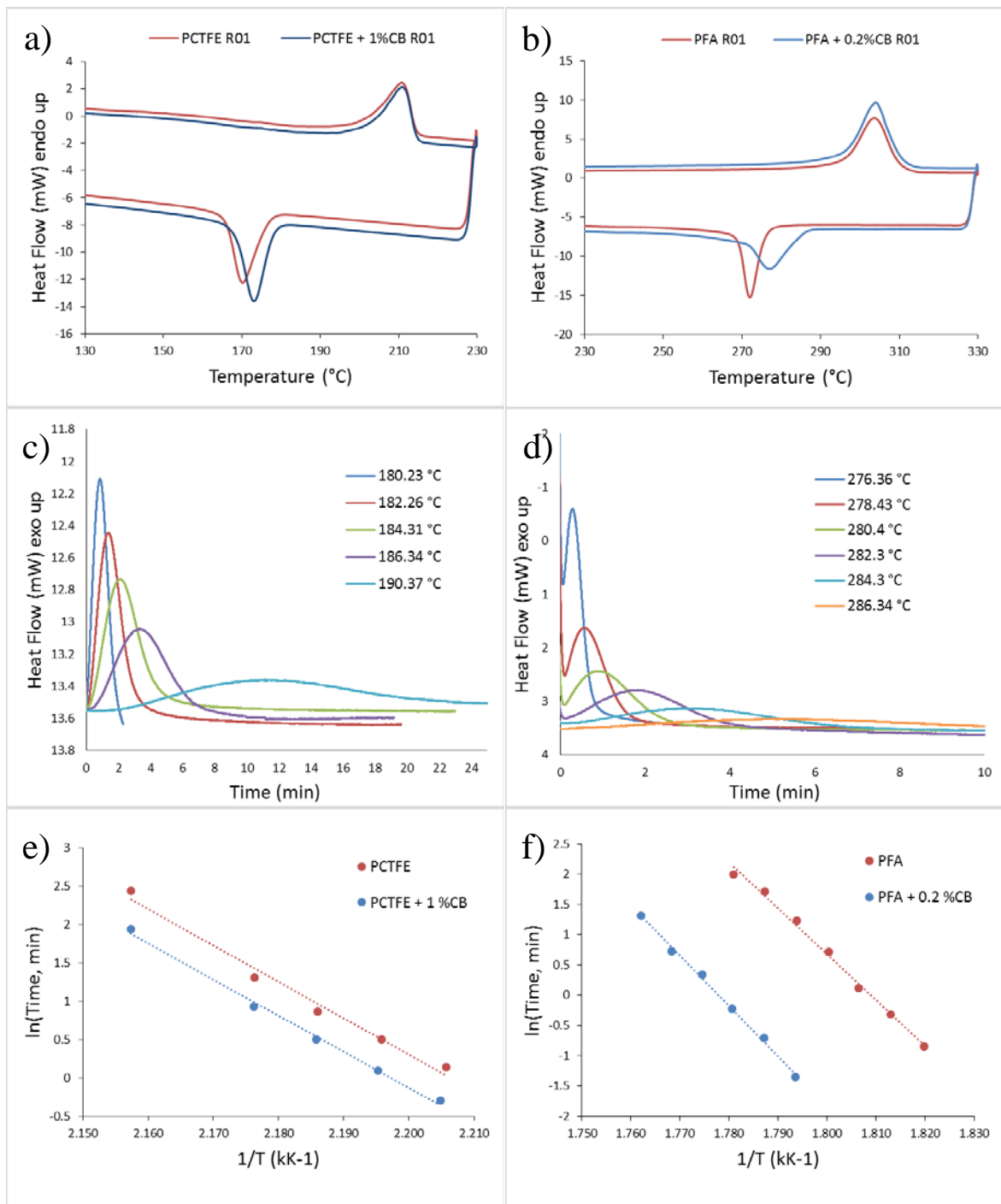
Figure 1 - DSC curves of PCTFE (left side) and PFA (right side). The first row shows the melting and crystallization temperature with a heating/cooling rate of 20 °C/min. The second row shows the isothermal crystallization at different temperatures for the pure powders. The third row shows the activation energy for the crystallization.

Particle size distribution

The average particle size quoted for the PCTFE powder was 150 μm but this value was found to be misleading. Initial dry analysis of the particle size distribution by volume gave results

already different to those stated by the supplier: D_{10} 1.39 µm, D_{50} 21.6 µm, D_{90} 158 µm. Nonetheless, the powder was too cohesive for that particle size range. SEM imaging showed that all the particles in the powder were roughly below 1 µm in size (Figure 2). Therefore, the dry analysis could not break the powder agglomerations effectively. To solve this issue, wet analyses were conducted. The wet analysis showed two peaks, the first at 0.4 µm (real size) and the second at 20 µm (agglomerations). The presence of the two peaks is likely due to the fact that the dispersing medium (water) was not ideal for PCTFE. The size of the second peak decreased with more mixing and sonication time suggesting that the dispersion improved with more time and mixing. Finally, the SEM imaging agreed with the peak at 0.4 µm (Figure 2).
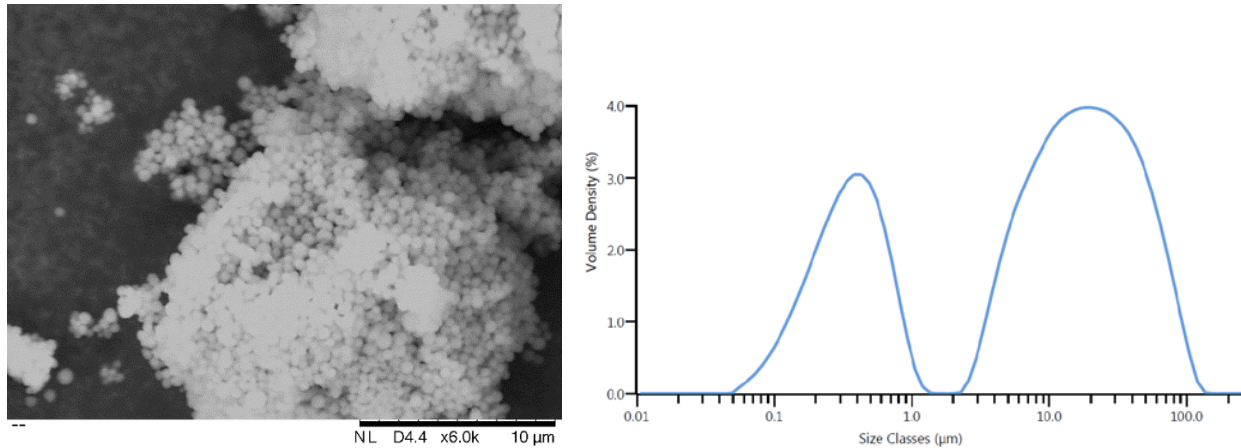

Figure 2- Left: SEM image of the PCTFE powder where only small particles of roughly 0.2-1 µm are observable. Right: PCTFE particle size distribution measured with a wet cell after 30 minutes of mixing and sonication.

The PFA powder had a particle size distribution by volume of D_{10} 8.03 µm, D_{50} 24.9 µm, D_{90} 51.2 µm. These values agreed with the values provided by the supplier and the SEM imaging (Figure 3). The particle size distribution by number was D_{10} 0.932 µm, D_{50} 1.30 µm, D_{90} 4.07 µm, showing that the majority of the particle were small and thus leading to cohesion.
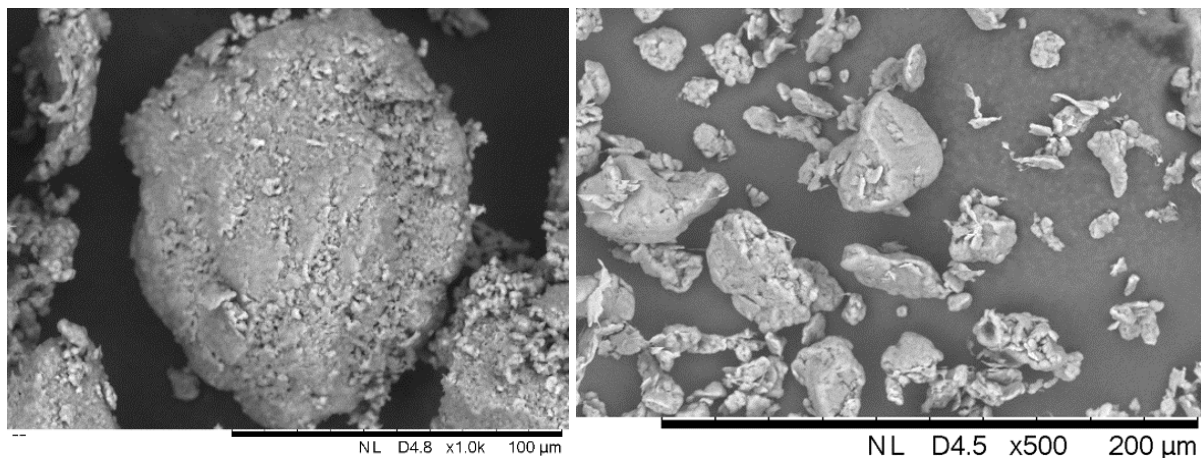

Figure 3- Left: SEM image of a PCTFE powder particle after 20 minutes at 250°C. Right: SEM image of the PFA powder.

FT4 Flowability study

The conditioned bulk density (CBD) results for the PCTFE powder are reported in Table 1 and Figure 4. The CBD of the virgin powder was 0.51 g/ml, 23.8% of the absolute density (2.13 g/ml), while the specific energy (SE) was 11.83 mJ/g. The use of a static eliminator did not visibly improve the CBD or SE. The thermal conditioning at 200-205-210 °C for 4h and 210 °C for 23h progressively improved the CBD to 0.54-0.57-0.60-0.62 g/ml, respectively. The SE showed a more marked decrease at 210 °C for 23h. The use of fumed nano-silica (NS) had a negative effect on the CBD, which decreased to 0.42 g/ml for 2 wt% NS; the SE also decreased to 8.2 mJ/g. The addition of carbon black (CB) showed drastic improvement to the CBD and SE. The CBD increased to 0.56-0.59-0.59-0.57 g/ml and the SE decreased to 5.50-3.69-3.35-3.50 mJ/g for 0.55-1-2-3 wt% CB, respectively. The improvements seemed to peak at 2 wt% CB after which they declined, indicating that this is the concentration with optimal coverage of the polymer particles. CB performed better than NS possibly because the NS did not disperse well or the loading used was too high. Another possible reason for the better performance seen with CB is that CB is a conductive material and can decrease the cohesion between particles caused by static charges.

A further test was to laser sinter the PCTFE 1 wt% CB powder in the P100 and then grind it. The parameters used were: 2 scans, laser power 2W, scan velocity 2000 mm/s, hatch spacing 0.05 mm. The powder produced showed a great improvement in CBD (0.82 g/ml, 38.6%) and a low SE (4.55 g/ml). This improvement was due to the increase in particle size.

Table 1 – Conditioned bulk density (CBD) and Specific Energy (SE) of PCTFE powders with and without additives and after thermal treatments. NS = fumed nano-silica, CB = carbon black.

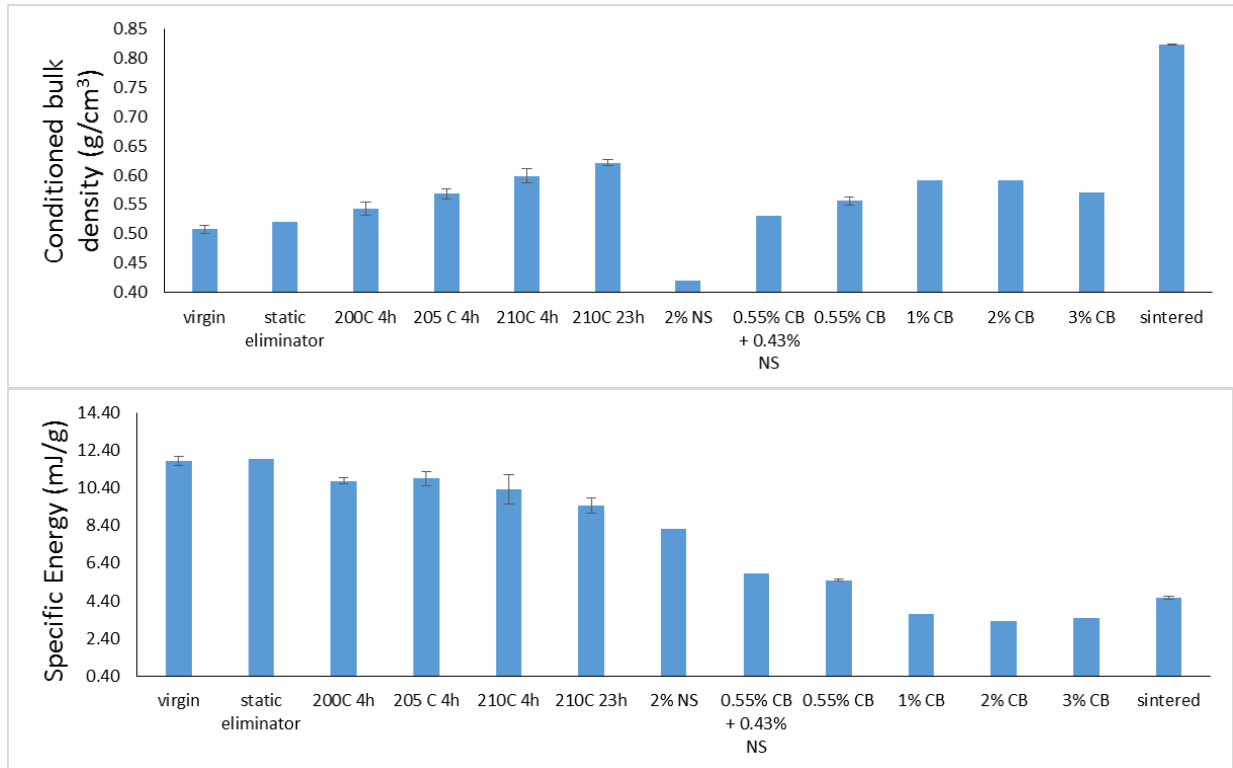|	CBD (g/ml)	std	SE (mJ/g)	std
virgin	0.51	0.01	11.83	0.23
static eliminator	0.52	/	11.95	/
200 °C, 4h	0.54	0.01	10.77	0.18
205 °C, 4h	0.57	0.01	10.89	0.39
210 °C, 4h	0.60	0.01	10.33	0.79
210 °C, 23h	0.62	0.01	9.46	0.41
2% NS	0.42	/	8.20	/
0.55% CB + 0.43% NS	0.53	/	5.85	/
0.55% CB	0.56	0.01	5.50	0.06
1% CB	0.59	/	3.69	/
2% CB	0.59	/	3.35	/
3% CB	0.57	/	3.50	/
sintered	0.82	0.00	4.55	0.07

Figure 4 - FT4 results for the PCTFE powder for different heat treatment and mixtures.

The FT4 findings were confirmed by experimental observations. Figure 5 shows how the PCTFE powder was very cohesive and not capable of forming a smooth layer inside of the P100. With the addition of 1 wt% CB, the powder was able to form smooth repeatable layers (Figure 5). Even though 2 wt% CB showed the best flowability in the FT4 study, 1 wt% CB was used to minimize possible negative effects on the properties of the final parts.
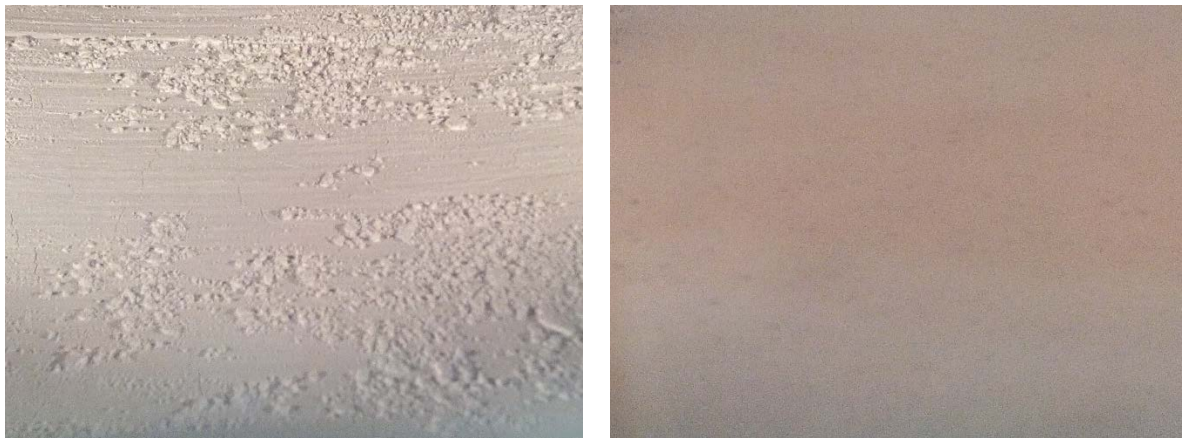

Figure 5 - Left: Neat PCTFE powder showing bad flowability. Right: PCTFE powder + 1 wt% carbon black showing improved flowability.

A similar study was done for PFA (Figure 6). The virgin powder had a CBD of 0.80 g/ml, 37.3% of the absolute density (2.15 g/ml), while the SE was 10.07 mJ/g. The virgin PFA powder

performed better than the virgin PCTFE powder due to its larger particle size distribution. The used powder (17 uses) did not show any visible change to the CBD or SE. The addition of carbon black showed an improvement to the CBD and SE. The CBD increased to 0.89 and 0.90 g/ml (41.9%) while the SE decreased to 5.52 and 3.57 mJ/g for 0.2 and 0.5 wt%, CB, respectively.
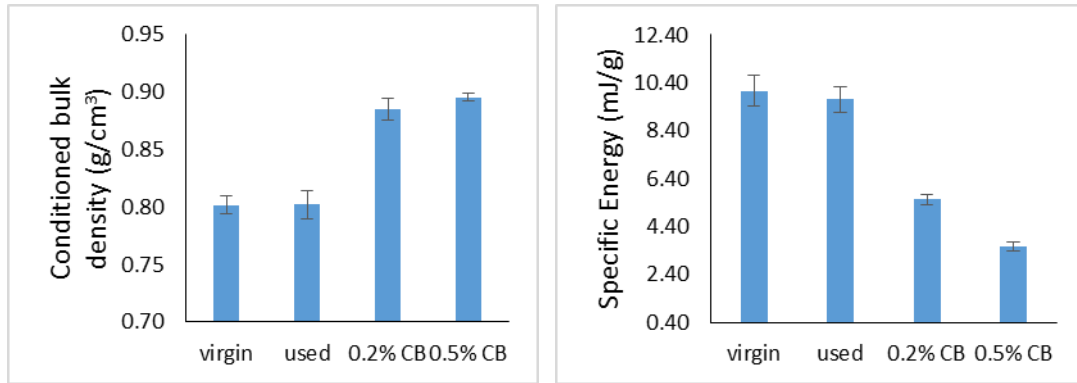

Figure 6 - FT4 results for the PFA powder for different mixtures.

While using the PFA powder in the P100, it was observed that the powder could form a smooth layer but only on the first layer (Figure 7). Nevertheless, the spreading of successive layers failed due to the cohesiveness of the powder. In fact, even when the powder seemed to be spreading well, nothing was being spread onto a layer until the powder bed decreased by roughly 7 layers (0.7 mm) and the powder was deposited all at once, as shown in Figure 7. Similar to the PCTFE powder, this issue was resolved with the addition of 0.4 wt% CB. A lower CB loading was required for PFA compared to PCTFE because of the larger particle size distribution of PFA as shown in the previous section. Under the SEM, the PFA powder looked like the thermally-treated PCTFE powder (Figure 3). This suggests that the PFA powder was produced in a similar manner and that thermal treatments could be an effective way to increase the particle size and improve flowability.
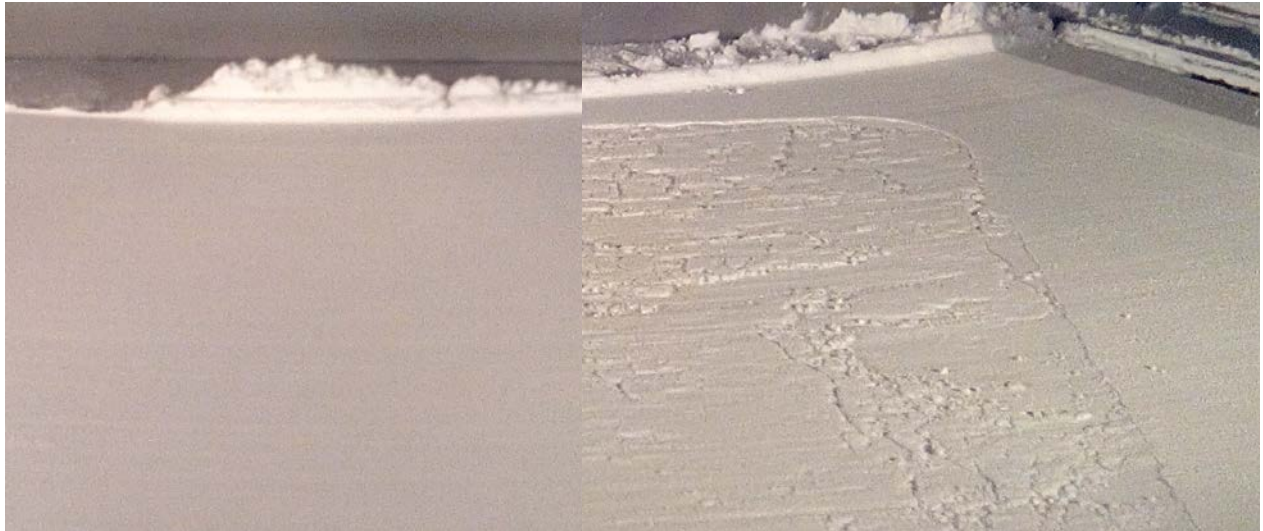
Figure 7 - PFA powder flow. Left: good powder flow for the first layer. Right: poor powder flow for successive layers.

Laser sintering PCTFE

As an initial test, the PCTFE powder was used as received without the addition of additives. A screening of the process parameters was conducted to obtain an outline of ideal conditions. It was observed that, at a powder bed temperature of 178 °C, energy densities roughly above 0.025 J/mm^2 would produce a white smoke due to the decomposition of the polymer. Figure 8 shows on the left a 20 x 20 mm square produced with 2 scans per layer (one in the X direction, one in the Y direction), 0.015 J/mm^2 energy density per scan, 6W laser power, 2000 mm/s scan speed, 0.2 mm hatch spacing, and 0.1 mm layer thickness. The samples were porous and brittle.

Figure 8 – Left: laser sintered PCTFE. Right: laser sintered PCTFE 1 wt% CB part, 20 x 20mm.

Table 1 shows the laser sintering experiments conducted on the PCTFE 1 wt% CB powder. The process was limited by the warping of the parts due to the relatively low powder bed temperature of 182 °C too close to the crystallization temperature (Figure 8). Therefore, the experiments were carried out to pinpoint the optimal laser parameters and scan strategies to minimize warping. While using a 3 W laser, 2000 mm/s scan speed, 0.02 mm hatch spacing, light smoke was observed and thus laser powers of 1 and 2 W were used for the remaining experiments.

The experiments were evaluated by counting the number of layers printed before catastrophic failure (the part touching the recoating blade). It was observed that:

- The number of layers before the parts would warp enough to touch the recoating blade decreased at higher scan numbers (the other parameters were kept constant) due to the higher degree of sintering as confirmed by SEM imaging.
- The Support (S) scan strategy consisted of scanning the surrounding powder with a low energy density scan before scanning the actual part. The number of layers printed before warping almost tripled compared to a Normal (N) scan with the same laser parameters, going from 4 to 11 layers. While the additional scanning was not strong enough to considerably sinter the powder, it might have mitigated the warping by dispersing it into a wider area and/or by lightly anchoring the sintered part to the powder bed.
- The Alternating (A) scan strategy introduced a waiting time between scans which causes the parts to cool down between successive scans. This decreased the amount of warping but it was likely caused by an overall lower degree of sintering.
- The combination of Alternating and Support (A + S) scan strategy did not seem to introduce any major improvements.

Table 2 – PCTFE 1 wt% CB laser sintering experiments. N = normal, S = Support, A = Alternating. The total ED is the ED of a single scan multiplied by the number of scans.

Type	Total ED (J/mm^2)	Number of scans per layer	Laser Power (W)	Scan Speed (mm/s)	Hatch Spacing (mm)	Layer Thickness (mm)	Number of layers before failing	Note
N	0.008	1	3	2000	0.2	0.05	N/A	Light smoke
N	0.008	3	1	2000	0.2	0.05	22	
N	0.010	2	2	2000	0.2	0.05	20+	Ran out of powder
N	0.015	3	2	2000	0.2	0.05	15	
N	0.020	4	2	2000	0.2	0.05	9	
N	0.030	6	2	2000	0.2	0.05	4	
S	0.030	6	2	2000	0.2	0.05	11	
A	0.030	6	2	2000	0.2	0.05	16	
A	0.030	12	1	2000	0.2	0.05	18	
A+S	0.030	12	1	2000	0.2	0.05	19	No improvements
N	0.020	2	1	2000	0.05	0.05	11	Warps from layer 1

In a further test, one of the printed parts was subject to an oven post-sintering step of 30 minutes at 250 °C. This thermal treatment increased the density of the printed part from ~35% to ~60%. The parts were no longer brittle and could be bent to angles greater than 90° without fracture. Higher densities may be achieved with longer residence times or higher temperatures.

Overall, the PCTFE powder had an acceptable powder flow when carbon black was added but it tended to warp after 10-20 layers due to the chamber temperature being too close to the crystallization temperature of the polymer. Furthermore, the viscosity was too high to form fully dense parts, the melt flow index of the PCTFE powder was 0.97 g/10min (information provided by the supplier) while a commercial PA powder (LS grade) has a MFI of ~ 50-60 g/10min [20].

Laser sintering PFA

The sintering of a single layer of the PFA powder revealed that the amount of warping was proportional to the degree of sintering and energy density (ED) except when the polymer was fully melted (Figure 9). This was likely due to the relatively high viscosity of the polymer and fast heating/cooling rates characteristic of the laser sintering process. It was found that this did not allow for the formation of a complete molten layer unless high EDs (with consequent decomposition) would be used. All the following experiments used a powder bed temperature of 182 °C. Figure 9 shows how the degree of sintering decreases at lower laser powers (lower ED). The parameters used to produce 20 x 20 mm parts were 18/10/5 W (from left to right), 2 scans, 2000 mm/s scan speed, 0.1 mm hatch spacing. When the samples were cleaned with isopropanol they appeared transparent (Figure 9 center). When a laser power of 18 and 26 W was utilized it caused smoking.
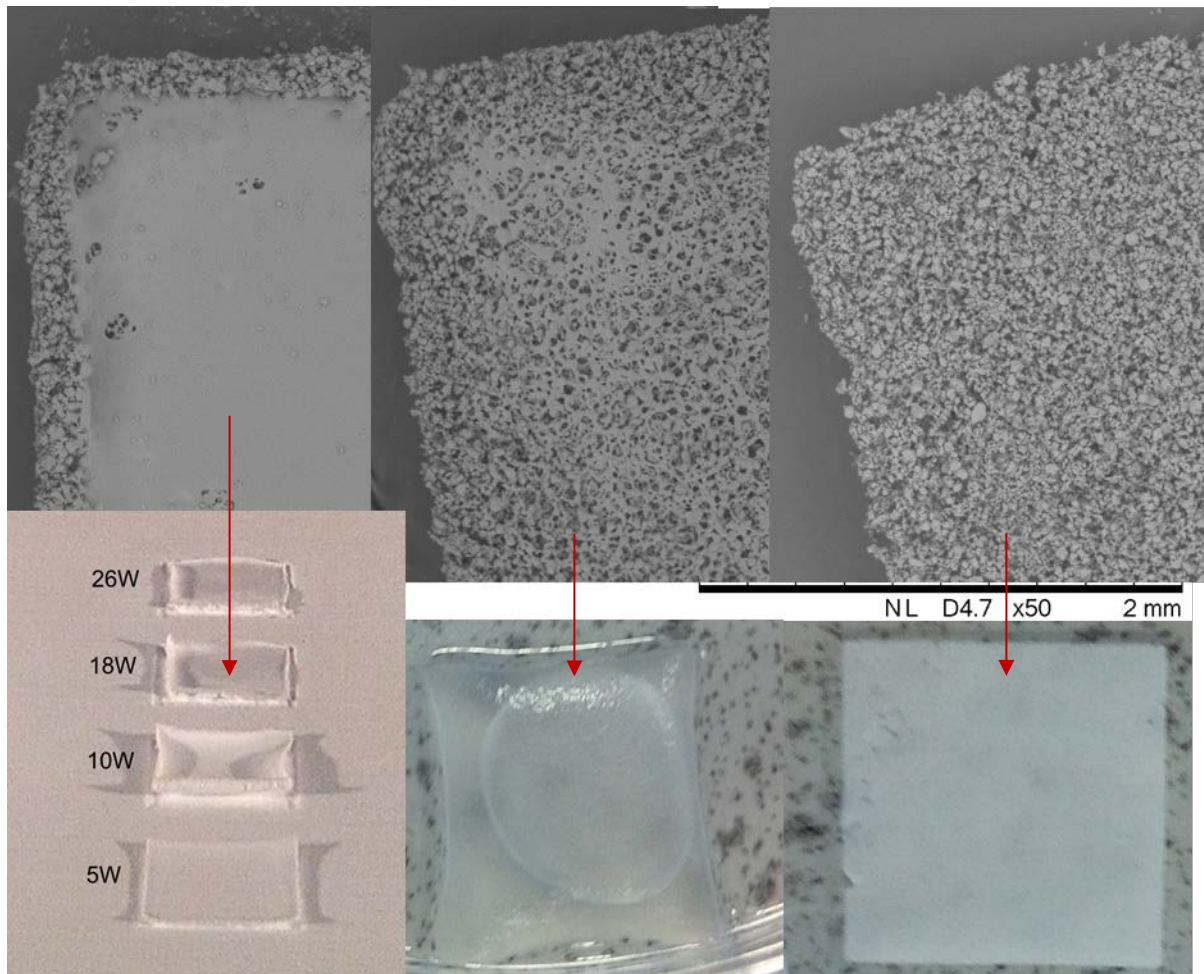

Figure 9 – Laser sintered PFA powder. As the laser powder decrease, the parts become more porous and fragile. 18/10/5 W from left to right (2 scans, 2000 mm/s scan speed, 0.1 mm hatch spacing).

The orientation of the part was also important as shown in Figure 10; the parts were scanned twice with the same parameters, once in the X direction (from bottom to top) and once in Y

direction (from right to left). This meant that at the end of the first scan (X), right before the second scan would start, the last area exposed to the laser was the top side. As the top side had less time to cool down, it was at a higher temperature during the Y scan, generating a hot spot. A higher temperature meant more sintering, which meant more warping (as observed in Figure 9 and from other experiments). When the sample was rotated by 45° the last part to be scanned in the first scan (X) was positioned in the middle of the next scan (Y), giving more uniform temperature distribution and warping. Nevertheless, the top right side still showed the presence of a smaller hot spot. The warping can be followed by looking at the shadows cast by the parts. When carbon black was used, the areas with a higher degree of sintering appeared darker (Figure 10). When more than two scans were used, two hot spots and preferential warping in opposite positions were present, one in the top right corner and one in the bottom left corner. When 2 scans in the X direction were used the parts showed uniform warping and color.
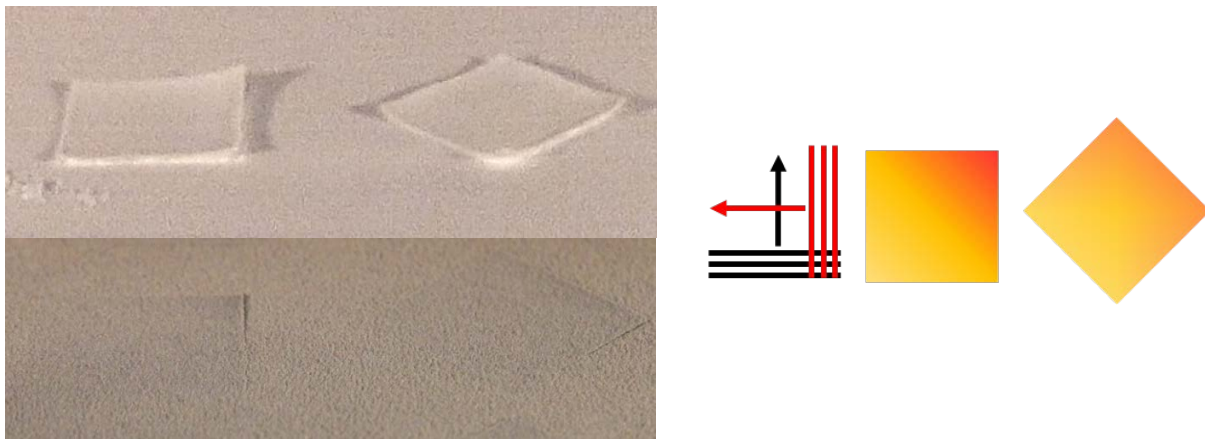

Figure 10 – Laser sintered PFA without (top left) and with carbon black (bottom left) highlighting the effect of scan strategy and part orientation on sintering and warping. The warping/sintering was stronger in areas corresponding to the hot spot (red area, top right corner). The parts are first scanned in X direction (from bottom to top) and then in the Y direction (right to left).

A further experiment is shown in Figure 11, where different hatch spacings (1.5-1-0.75-0.5 mm) were printed at 20 W, 2000 mm/s, 1 scan in the X direction, 1 scan in the Y direction, and single layer. The SEM showed the presence of gaps for hatch spacings of 1.5-1-0.75 mm but not for 0.5 mm (nonetheless, it was possible to see grids with the naked eye). The track width (~350 μm) was roughly the same in the X and Y direction with a hatch spacing of 1.5 mm, but the Y track was thicker (~400 μm) when a hatch spacing of 0.75 mm was used. This was probably because the Y scan was done after the X scan, which increased the temperature of the powder in the surrounding area (thus, it is like processing at a higher powder bed temperature). When the hatch spacing was wider than 0.5 mm, the parts showed more homogenous shrinkage and no warping.
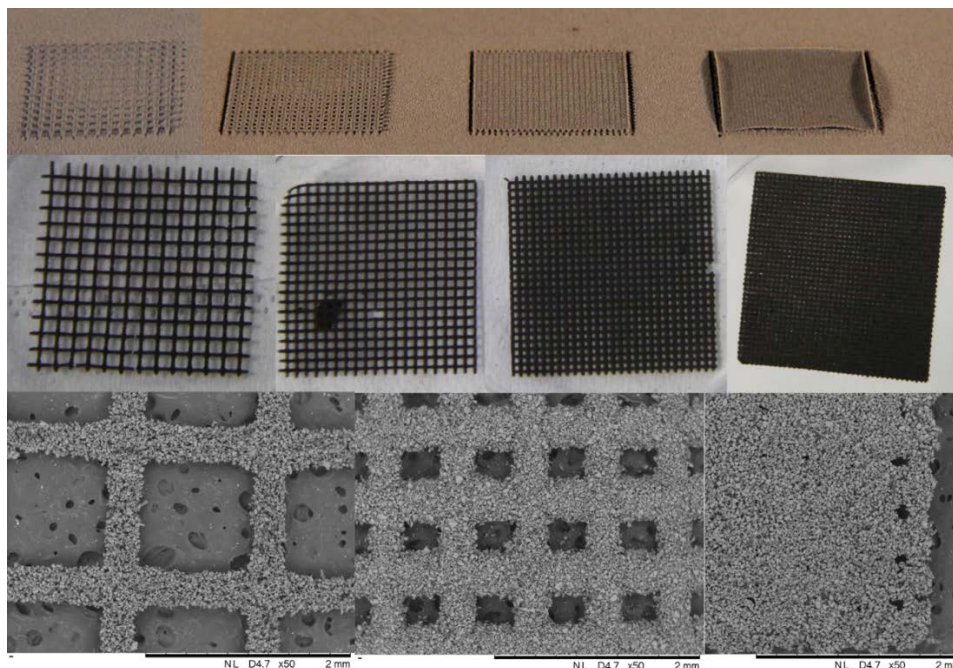
Figure 11 – Laser sintered PFA. Single scan in the X and Y direction with hatch spacings of 1.5-1-0.75-0.5 mm, left to right. The SEM shows hatch spacings of 1.5-0.75-0.5 mm.

Warping was the main failure mechanism at this stage; thus, an aluminum plate (100 x 100 x 8 mm) covered in blue masking tape was introduced in the center of the build chamber and used as build plate. The idea behind it was that during the sintering of the first layer, the melted powder would stick to the blue masking tape decreasing or eliminating the warping [21]. The technique partially worked as it was possible to print 10-15 layers before running out of powder and with only minor warping (Figure 12d). The minor warping is due to the weak bonding between blue masking tape and polymer.

A lower CB loading was also tested. PFA with 0.2 wt% CB showed a smooth layer formation similar to that of 0.4 wt% CB. With this formulation, a single layer 100 x 100 mm sheet/membrane with a thickness of ~150 μm and porosity of ~60% was printed (Figure 12a). The parameters utilized were: single scan in the X direction; 18 W laser power, 2000 mm/s scan speed; and 0.2 mm hatch spacing. The sheet warped soon after printing, as seen in Figure 12a. After a thermal treatment of 3 hours at 260 °C to relieve the residual stresses, the film became flat (Figure 12c). To the touch, the sheet had a fabric feeling and was extremely flexible. By lifting and looking through the sheet, CB agglomerates were visible (Figure 12b). These agglomerations were due to sub-optimal mixing. The sheet was porous but a water drop had a high contact angle and could not penetrate, as shown in Figure 12a. On the other hand, isopropanol, which has a lower surface tension than water, went through the sheet. A drop of water contaminated with isopropanol also went through the membrane.
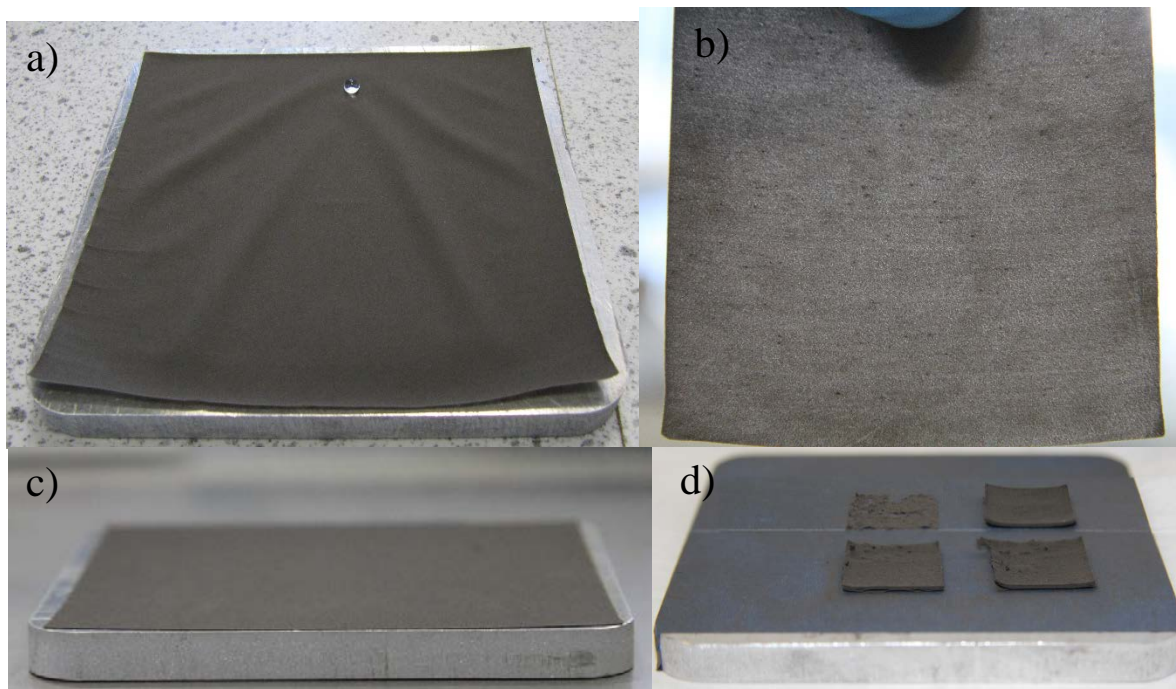
Figure 12 – Laser sintered PFA 0.2 wt% CB sheet/membrane as printed (a) and after 3hours at 260 °C (c). (b) Visible agglomerations of carbon black. (d) Blue tape used as build plate.

Discussion

The thermal characterization of the PCTFE and PFA powder showed how the presence of carbon black (CB) increases the crystallization temperature, and consequently the crystallization speed from the melt polymers. Therefore, increasing the minimum powder bed temperature required to avoid warping. PCTFE likely requires a powder bed temperature above 190 °C: at that temperature, 50% of the crystallization happened after 11.4 and 6.9 minutes when PCTFE was used without and with 1 wt% CB, respectively. Similarly, PFA likely requires a powder bed temperature above 288 °C: at that temperature, 50% of the crystallization happened in less than 10 minutes for both neat PFA and PFA with 0.2 wt% CB.

The PCTFE had a particularly small particle size distribution (<1 μm) and required a flowing agent to spread correctly in the P100. The chosen flowing agent was carbon black (CB). Even though 2 wt% CB showed the best flowability in the FT4 study, 1 wt% CB was used to minimize possible negative effects on the properties of the final parts. Another flowing agent utilized was fumed nano-silica (NS) but it did not perform as well as CB. This may be because the NS did not disperse well or the loading used was too high. Another possible reason for the better performance seen with CB is that CB is a conductive material and can decrease the cohesion between particles caused by static charges.

A further way to improve the flowability of the PCTFE powder was to heat the powder at temperatures above 200 °C for several hours. The longer the residence time and the higher the temperature, the greater the improvement in flowability. Another method of thermal treatment was to use the CO_2 laser of the Formiga P100 to sinter a layer of powder and subsequently grind the produced parts. The newly obtained powder showed an increase in particle size and a remarkable increase in conditioned bulk density to 0.82 g/ml from the 0.51 g/ml of the virgin powder, 38.6% and 23.8% of the absolute density, respectively. The PFA had a larger particle size distribution and,

under the SEM, the powder particles looked similar to the thermally-treated PCTFE particles. This suggests that the PFA powder was produced in a similar way: with a thermal treatment step. Despite the larger particle size distribution, the PFA powder still required the use of CB to have good flowability but in a smaller amount compared to PCTFE: just 0.5 wt% instead of 1 wt%. Loadings as low as 0.2 wt% also showed satisfactory flowing properties. No visible changes were observed between the virgin and used powder.

The sintered PCTFE parts showed a tendency to warp after 10-20 layers depending on the parameters and scan strategies utilized. This was caused by the powder bed temperature (~182 °C) being too close to the crystallization temperature of the polymer (170 °C). The presence of CB increased the absorbance of the CO_2 laser, as evidenced by how the powder started smoking when exposed to lower energy densities, from ~0.025 to ~0.008 J/mm^2. Optimized scanning strategy lead to a marked increase in printable layers before the parts would warp enough to touch the recoating blade. The reduced warping was likely due a lower degree of sintering when a delay was introduced between scans on the same layer and due a support effect from the surrounding powder when the part and surrounding powder were exposed to a low energy scan before scanning the actual part. The printed parts were brittle but a post sintering step at 250°C for 30 minutes increased the mechanical properties of the parts and density from ~35% to 60%. Higher densities may be achieved with longer residence time or higher temperatures in the oven.

The sintered PFA parts showed a tendency to warp instantly on the first layer because of the big thermal jump between the crystallization temperature (271.93 °C) and powder bed temperature (182 °C). The warping can be mitigated by using blue masking tape on the build plate. More than 15 layers were printed before running out of powder which meant that more layers could have been printed. Warping was absent when grid structures with a hatch spacing roughly above 0.7 mm were produced. The grids shrank uniformly in all directions. Thin porous membranes can also be produced. The membranes were initially warped but a heat treatment at 260 °C flattened them. This suggests that a powder bed temperature of 260 °C could avoid warping. In future works, the density, porosity and pore size of the membranes may be tuned by changing the laser parameters or with a post-sintering step in an oven. The thin membranes also revealed agglomerations of CB and they may be used to assess the quality/performance of different mixing methods.

Overall, PCTFE and PFA showed potential for laser sintering and can already be used to produce thin membranes. A process that uses a relatively low powder bed temperature can bring considerable economic advantages both on equipment investment and power consumption. Nonetheless, higher powder bed temperatures and/or support structures might be required to print bigger and more complex parts.

Conclusion

This study showed how the presence of carbon black (CB) increases the crystallization temperature, and consequently the crystallization speed from the melt polymers, increasing the minimum powder bed temperature required to avoid warping. The flowability of the powders was shown to be improved by thermal conditioning and addition of CB. The addition of fumed nano-silica (NS) did not have a beneficial effect on the conditioned bulk density (CBD) of the PCTFE power. Higher temperatures and longer residence times in the oven were shown to improve the CBD. Similar effects were obtained by using the CO_2 laser to sinter the powder and then grinding it with a pestle and mortar.

The PCTFE powder had acceptable powder flow when carbon black (1 wt%) was added but it tended to warp after 10-20 layers due to the powder bed temperature (182 °C) being too close to the crystallization temperature of the polymer (170 °C). Furthermore, the viscosity was too high

to form fully dense parts, the Melt Flow Index of the PCTFE powder was 0.97 g/10min. The printed parts were brittle but their properties can be improved with a post-sintering step in the oven.

The PFA powder showed a better flowability compared to the PCTFE powder because of its larger particle size distribution but it still required CB. A smaller amount of CB (0.2 wt%) was required compared to PCTFE. Similarly to PCTFE, warping was the major issue encountered but it could be mitigated by using blue masking tape on a build plate. Nonetheless, printing single layer parts that could be used as membranes was possible. The use of blue masking tape on a build plate enabled printing of multiple layers.

Acknowledgements

References

[1]   R. S. Evans, D. L. Bourell, J. J. Beaman, and M. I. Campbell, "SLS materials development method for rapid manufacturing," in *Proceedings SFF Symposium, Austin (TX), USA*, 2005, pp. 184–196.

[2]   R. D. Goodridge, C. J. Tuck, and R. J. M. Hague, "Laser sintering of polyamides and other polymers," *Prog. Mater. Sci.*, vol. 57, no. 2, pp. 229–267, Feb. 2012.

[3]   J. G. Drobny, *Technology of Fluoropolymers*, 2nd ed. Boca Raton: CRC Press Taylor & Francis Group, 2009.

[4]   D. W. Smith, S. T. Iacono, and S. S. Iyer, *Handbook of fluoropolymer science and technology*. John Wiley & Sons, 2014.

[5]   D. A. Dixon, B. E. Smart, P. J. Krusic, and N. Matsuzawa, "Bond energies in organofluorine systems: applications to Teflon® and fullerenes," *J. Fluor. Chem.*, vol. 72, no. 2, pp. 209–214, Jun. 1995.

[6]   D. Thuau, K. Kallitsis, F. D. Dos Santos, and G. Hadziioannou, "All inkjet-printed piezoelectric electronic devices: energy generators, sensors and actuators," *J. Mater. Chem. C*, vol. 5, no. 38, pp. 9963–9966, 2017.

[7]   R. I. Haque, R. Vié, M. Germainy, L. Valbin, P. Benaben, and X. Boddaert, "Inkjet printing of high molecular weight PVDF-TrFE for flexible electronics," *Flex. Print. Electron.*, vol. 1, no. 1, p. 15001, 2015.

[8]   O. Pabst, S. Hölzer, E. Beckert, J. Perelaer, U. S. Schubert, R. Eberhardt, and A. Tünnermann, "Inkjet printed micropump actuator based on piezoelectric polymers: Device performance and morphology studies," *Org. Electron.*, vol. 15, no. 11, pp. 3306–3315, 2014.

[9]   O. Pabst, J. Perelaer, E. Beckert, U. S. Schubert, R. Eberhardt, and A. Tünnermann, "All inkjet-printed piezoelectric polymer actuators: Characterization and applications for micropumps in lab-on-a-chip systems," *Org. Electron.*, vol. 14, no. 12, pp. 3423–3429, Dec. 2013.

[10]   U. S. Bhansali, M. A. Khan, and H. N. Alshareef, "Organic ferroelectric memory devices with inkjet-printed polymer electrodes on flexible substrates," *Microelectron. Eng.*, vol. 105, pp. 68–73, May 2013.

[11]   D. A. Porter, T. V. T. Hoang, and T. A. Berfield, "Effects of in-situ poling and process parameters on fused filament fabrication printed PVDF sheet mechanical and electrical properties," *Addit. Manuf.*, vol. 13, pp. 81–92, 2017.

[12]   C. Lee and J. A. Tarbutton, "Electric poling-assisted additive manufacturing process for PVDF polymer-based piezoelectric device applications," *Smart Mater. Struct.*, vol. 23, no. 9, p. 95044, 2014.

[13]   W. Huang, P. Wu, P. Feng, Y. Yang, W. Guo, D. Lai, Z. Zhou, X. Liu, and C. Shuai, "MgO whiskers reinforced poly(vinylidene fluoride) scaffolds," *RSC Adv.*, vol. 6, no. 110, pp. 108196–108202, 2016.

[14]   C. Shuai, W. Huang, P. Feng, C. Gao, D. Gao, Y. Deng, Q. Wang, P. Wu, and X. Guo, "Nanodiamond reinforced polyvinylidene fluoride/bioglass scaffolds for bone tissue engineering," *J. Porous Mater.*, vol. 24, no. 1, pp. 249–255, 2017.

[15]   "3M pioneers 3D printing with PTFE." [Online]. Available: https://www.3m.co.uk/3M/en_GB/design-and-specialty-materials-uk/products/full-story/?storyid=238bb6ed-2857-4929-93c5-a1c9cc684776. [Accessed: 27-Jun-2018].

[16]   Conservation and Art Materials Encyclopedia Online (CAMEO), "Polychlorotrifluoroethylene." [Online]. Available: http://cameo.mfa.org/wiki/Polychlorotrifluoroethylene. [Accessed: 12-Feb-2016].

[17]   AZO Materials, "Polychlorotrifluoroethylene (PCTFE) - Supplier Data by Goodfellow." [Online]. Available: https://www.azom.com/article.aspx?ArticleID=2342. [Accessed: 28-Jun-2018].

[18]   S. Ziegelmeier, F. Wöllecke, C. Tuck, R. D. Goodridge, and R. Hague, "Characterizing the bulk & flow behaviour of LS polymer powders," in *Proceedings SFF Symposium*, 2013.

[19]   G. M. Vasquez, C. E. Majewski, B. Haworth, and N. Hopkinson, "A targeted material selection process for polymers in laser sintering," *Addit. Manuf.*, vol. 1, pp. 127–138, 2014.

[20]   K. Dotchev and W. Yusoff, "Recycling of polyamide 12 based powders in the laser sintering process," *Rapid Prototyp. J.*, vol. 15, no. 3, pp. 192–203, May 2009.

[21]   T. NIINO, H. HARAGUCHI, Y. ITAGAKI, S. IGUCHI, and M. HAGIWARA, "Feasibility study on plastic laser sintering without powder bed preheating," in *Solid Freeform Fabrication Symposium*, 2011, vol. 20, pp. 0–5.